7. Z.P. Wang, J. Kelly, and P.S. Hall, Reconfigurable bandstop filter with wide tuning range, Electron Lett 46 (2010), 771–772.
8. L. Matekovits, M. Heimlich, and K. Esselle, Tunable periodic microstrip structure on GaAs wafer, Prog Electromagn Res 97 (2009), 1–10.
9. .D.N.P. Thalakotuna, L. Matekovits, K.P. Esselle, and M. Heimlich, Tunable periodic structures, In: 5th European Conference on Antennas and Propagation, EUCAP 2011, Rome, Italy, April 10–15, 2011, pp. 1118–1120.
10. D.N.P. Thalakotuna, L. Matekovits, M. Heimlich, K. Esselle, and S.G. Hay, Placement strategies for active devices and modelling of a 1D tunable EBG structure, J Electromagn Waves Appl 25 (2011), 1740–1751.
11. J.D. Joannopoulos, S.G. Johnson, J.N. Winn, and R.D. Mede, Photonic crystals–molding the flow of light, Princeton University Press, Princeton, NJ, 2008.

PLANAR, LIGHTWEIGHT, CIRCULARLY POLARIZED CROSSED DIPOLE ANTENNA FOR HANDHELD UHF RFID READER

Son Xuat Ta,[1] Hosung Choo,[2] and Ikmo Park[1]
[1] Department of Electrical and Computer Engineering, Ajou University, 5 Woncheon-dong, Youngtong-gu, Suwon 443-749, Korea; Corresponding author: ipark@ajou.ac.kr
[2] School of Electronics and Electrical Engineering, Hongik University, 72-1 Sangsu-dong, Mapo-gu, Seoul 121-791, Korea

Received 5 December 2012

ABSTRACT: *A planar, lightweight, crossed dipole antenna with circularly polarized (CP) radiation is introduced for application in a radiofrequency identification handheld reader at ultrahigh frequency bands. The dipoles cross through a 90° phase-delay line of a vacant-quarter printed ring that enables broadband characteristic in terms of impedance matching and 3-dB axial ratio (AR) bandwidths. Four printed inductors are symmetrically inserted into the dipole arms whose ends are barbed to achieve a compact size. A sample antenna with a size of 60 × 60 × 0.508 mm and weight of 3.6 g is designed, fabricated, and measured. The proposed antenna yields an impedance bandwidth of 851–941 MHz for $|S_{11}| < -10$ dB and a 3-dB AR bandwidth of 902–921 MHz. At 910 MHz, the antenna radiates bidirectional CP waves with a gain of 1.4 dBic and an AR of 1.1 dB.* © 2013 Wiley Periodicals, Inc. Microwave Opt Technol Lett 55:1874–1878, 2013; View this article online at wileyonlinelibrary.com. DOI 10.1002/mop.27674

Key words: *ultrahigh frequency radiofrequency identification; handheld reader; circular polarization; printed inductor; barbed dipole; phase-delay line*

1. INTRODUCTION

Recently, the radiofrequency identification (RFID) technology in the ultrahigh frequency (UHF) band has been applied to many service industries, manufacturing companies, transportation management, and distribution logistics [1]. An RFID system generally consists of a tag, a reader, and a data processing system. Linearly polarized dipoles of various shapes are chosen for UHF RFID tag antennas [2–5] owing to their compact size, light weight, and low cost. On the other hand, the RFID reader antennas are usually designed with circularly polarized (CP) radiation to increase orientation diversity and to reduce polarization mismatch. The CP stacked patch antennas [6,7] with a broad bandwidth and low cost have been popularly chosen for UHF RFID readers. However, the bulky configurations of these antennas are not desirable for handheld devices because they require a lightweight CP antenna with a low profile and small size. Various types of antennas with a planar structure and CP radiation for UHF RFID handheld and portable readers have been reported, including microstrip antennas [8,9], phase-delay fed antennas [10,11], and slot antennas [12,13]. However, the aforementioned antennas are still heavy (>10 g) owing to the use of a thick high-density substrate or a multilayer substrate.

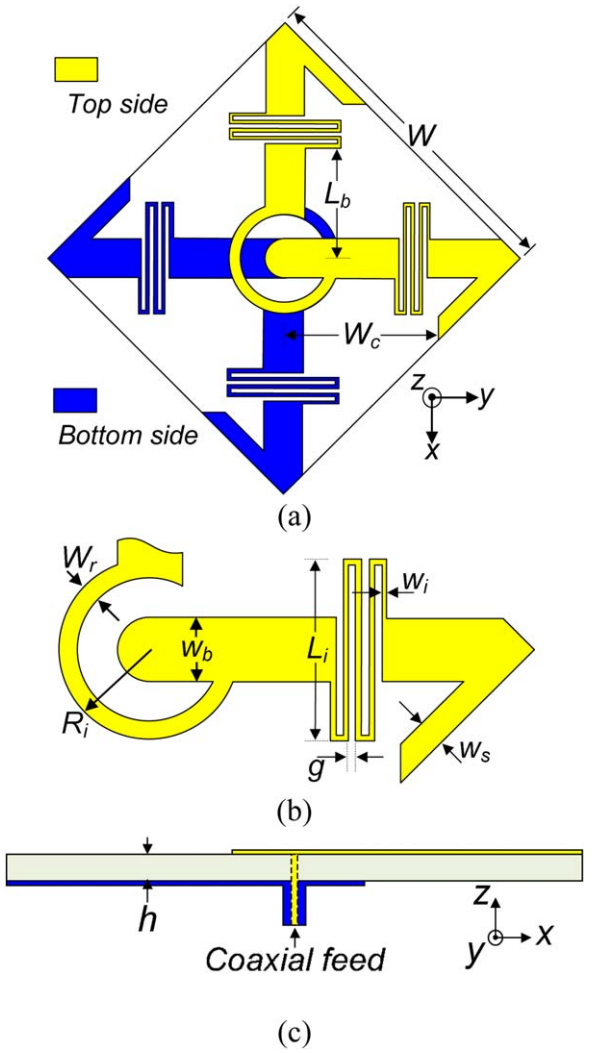

Figure 1 Planar crossed barbed dipole. (a) Top view. (b) Expanded view of the dipole arm with vacant-quarter printed ring. (c) Side view. [Color figure can be viewed in the online issue, which is available at wileyonlinelibrary.com]

This article proposes a planar, lightweight, crossed dipole antenna that exhibits CP radiation and broad bandwidth at the UHF RFID band. The antenna is printed on both sides of a thin substrate with low density to achieve a light weight. The feeding structure used in the proposed design is based on the 90° phase-delay line of a vacant-quarter printed ring reported in Ref. 14. The proposed design uses two techniques to reduce the size, namely, the use of printed inductors and the barbed shape at the end of the dipole arms.

2. ANTENNA DESIGN

Figure 1 shows the configuration of the planar crossed dipole antenna. The antenna was built on both sides of a 60 × 60 mm Rogers RO4003 substrate with a dielectric constant of 3.38, a

loss tangent of 0.0027, and a thickness of 0.508 mm. The antenna was composed of two dipoles and fed by a 50-Ω coaxial cable. A vacant-quarter printed ring was used as the 90° phase-delay line to generate the CP radiation. The outer conductor of the coaxial cable was welded to the crossed arms at the bottom side of the substrate, and the inner conductor of the coaxial cable was extended through the substrate to feed the crossed dipole at the top side. To reduce the dipole length, a printed inductor was inserted in each dipole arm whose end was barbed. The printed inductor with a trace width w_i, length L_i, and gap size g_i was placed at a distance L_b from the center of the antenna, as shown in Figure 1(b). An Ansoft high-frequency structure simulator (HFSS) was used to investigate the antenna characteristics. The optimized antenna design parameters were chosen for broad bandwidth in terms of both the −10 dB reflection coefficient and the 3-dB axial ratio (AR) as follows: $W = 60$ mm, $W_c = 27$ mm, $R_i = 10$ mm, $W_r = 2$ mm, $W_b = 8$ mm, $L_b = 18$ mm, $L_i = 20$ mm, $g_i = 0.8$ mm, $w_i = 0.6$ mm, $W_s = 3$ mm, and $h = 0.508$ mm.

3. PARAMETRIC STUDY

The vacant-quarter printed ring was used not only to generate CP radiation but also to obtain the broadband characteristic.

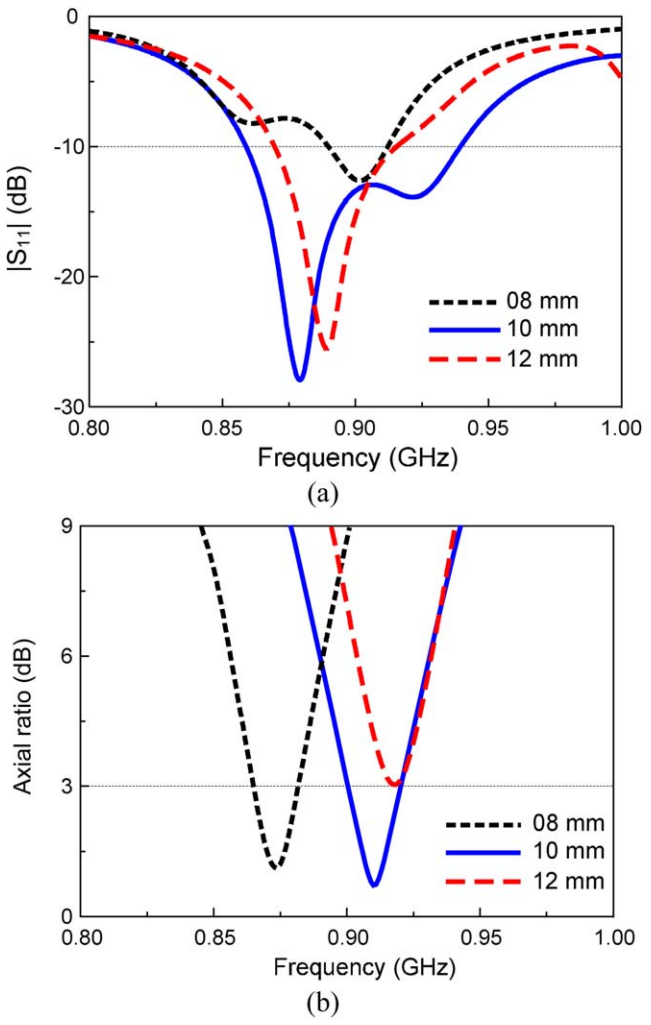

Figure 2 Simulated (a) $|S_{11}|$ and (b) AR as a function of the frequency for different radii R_i of the printed ring. [Color figure can be viewed in the online issue, which is available at wileyonlinelibrary.com]

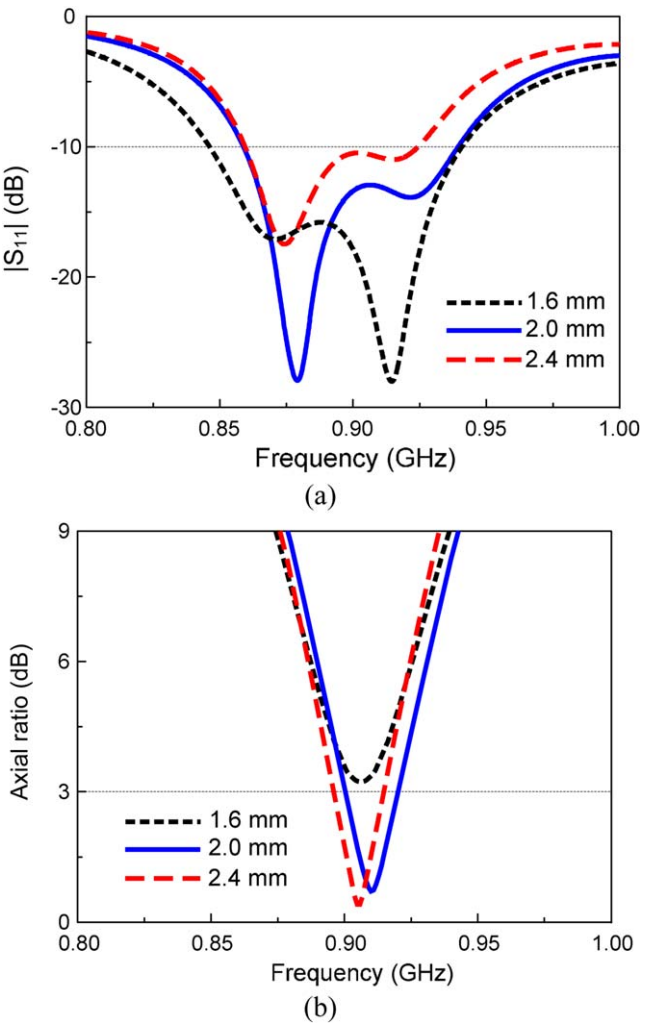

Figure 3 Simulated (a) $|S_{11}|$ and (b) AR as a function of the frequency for different widths W_r of the printed ring. [Color figure can be viewed in the online issue, which is available at wileyonlinelibrary.com]

These two properties can be clearly observed in Figures 2 and 3, which show the simulated $|S_{11}|$ and AR, respectively, of the proposed antenna as a function of the frequency for different radii (R_i) and widths (W_r) of the printed ring. Figure 2 shows that when the radius of the ring (R_i) was varied from 8 to 12 mm in 2 mm steps with the other design parameters given in Section 2 fixed, the reflection coefficient was significantly affected [Fig. 2(a)], whereas the CP center frequency increased [Fig. 2(b)]. Here, the CP center frequency was defined as the frequency with the minimum AR. $R_i = 10$ mm offered the optimized results in terms of broad impedance matching and 3-dB AR bandwidths, as well as minimum AR. When the width of the printed ring (W_r) was varied from 1.6 to 2.4 mm in 0.4 mm steps, the impedance matching bandwidth became narrow [Fig. 3(a)], whereas the CP center frequency slightly changed; however, the CP radiation improved in terms of the minimum AR [Fig. 3(b)]. In addition, the HFSS simulations showed that the antenna with $W_r < 1.7$ mm yielded an AR > 3 dB, and $W_r = 2$ mm showed the widest 3-dB AR bandwidth.

Figure 4 shows the simulated current distribution of the proposed antenna at 910 MHz for the two phase angles of 0 and 90°. The vertically oriented dipole arms worked at the 0° phase angle, whereas the horizontally oriented dipole arms worked at the 90° phase angle. This arrangement explained the CP

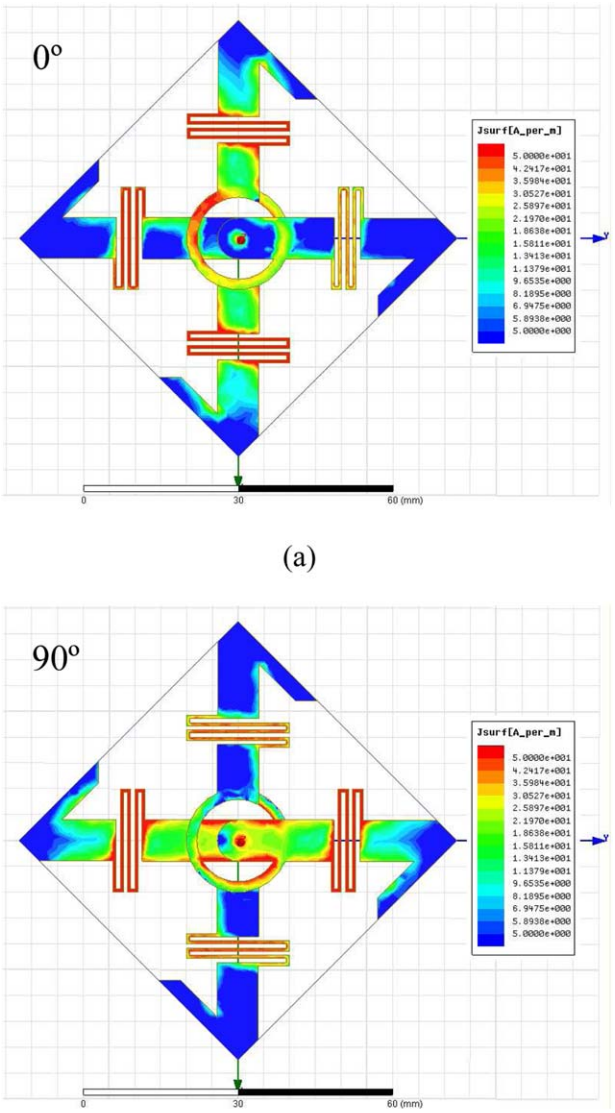

(a)

(b)

Figure 4 Simulated current distribution of the proposed antenna at 910 MHz for two phase angles: (a) 0° and (b) 90°. [Color figure can be viewed in the online issue, which is available at wileyonlinelibrary.com]

radiation behavior of the crossed barbed dipole antenna. Additionally, strong currents were distributed on the printed inductors because their trace width is much narrower than the width of the dipole arm. The above property indicated that the insertion of printed inductors significantly affected the antenna characteristics. In addition, the effects of the starting position (L_b) of the printed inductors on the antenna characteristics were also studied and are shown in Figure 5. When L_b was varied from 16 to 20 mm in increments of 2 mm, the resonant and CP center frequencies increased. This result indicated that the operating frequency of the proposed antenna can be controlled by the starting position of the printed inductors.

4. SIMULATION AND MEASUREMENT RESULTS

The planar crossed dipole antenna was fabricated on both sides of a Rogers RO4003 substrate with a copper thickness of 20 μm and a density of 1.79 g/mm^3 via a standard etching technology. The sample antenna with a size of 60 × 60 × 0.508 mm and a weight of 3.6 g was constructed, as shown in Figure 6(a). An Agilent N5230A network analyzer and a 3.5-mm coaxial calibration standard GCS35M were used for the reflection coefficient measurement of the antenna. Another Agilent E8362B network analyzer and two identical standard horn antennas were used for the radiation pattern measurements. The two horn antennas (one for transmitting and one for receiving) were initially connected to the two ports of the network analyzer for calibration. The receiving horn antenna was then replaced with the proposed antenna. The antenna was then mounted on a foam rack and fixed using thin tapes; the measurements were subsequently conducted in an anechoic chamber with a dimension of 15.2 m (W) × 7.9 m (L) × 7.9 m (H). In the measurement process, the transmitting antenna was fixed, whereas the receiving antenna was rotated from −180 to 180° in 1° increments at an angular velocity of 3°/s. Figure 6(b) shows the $|S_{11}|$ and AR of the proposed antenna, and a good agreement between the simulations and measurements can be observed. The measured bandwidth was 851–941 MHz for $|S_{11}| < -10$ dB, whereas the simulated bandwidth was 860–940 MHz. The measured 3-dB

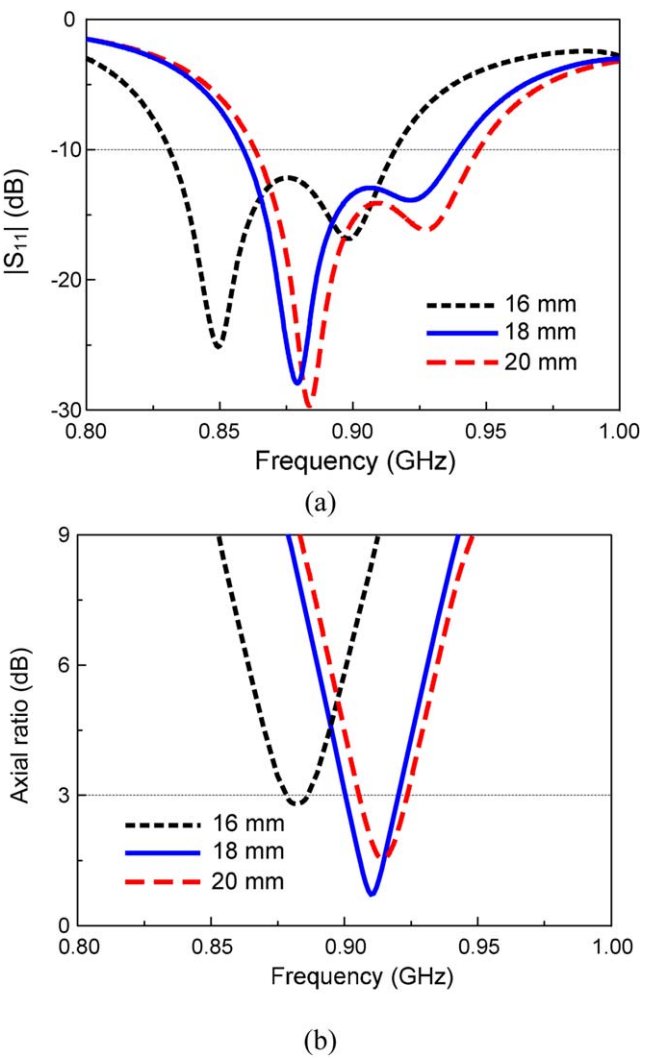

(a)

(b)

Figure 5 Simulated (a) $|S_{11}|$ and (b) AR as a function of the frequency for different starting points (L_b) of the printed inductor. [Color figure can be viewed in the online issue, which is available at wileyonlinelibrary.com]

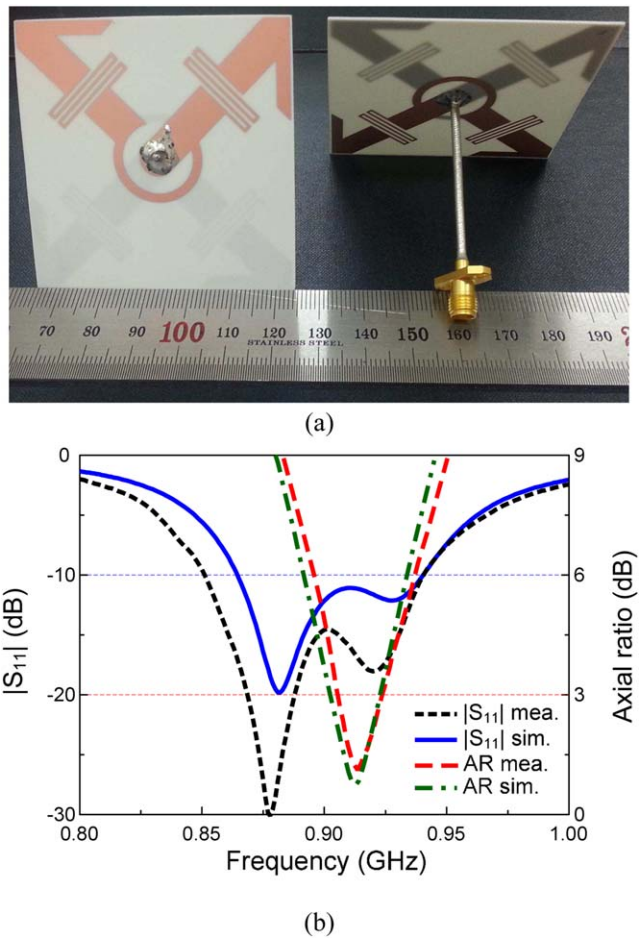

Figure 6 (a) Fabricated antennas and (b) $|S_{11}|$ and AR. [Color figure can be viewed in the online issue, which is available at wileyonlinelibrary.com]

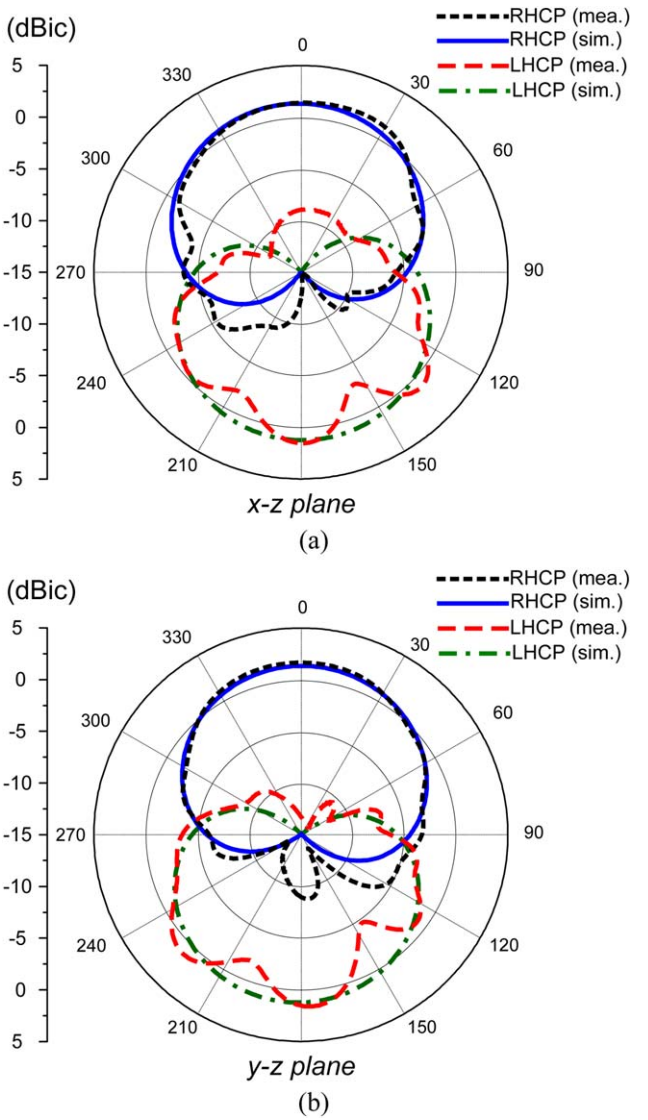

Figure 7 Radiation pattern of the antenna at 910 MHz. (a) *x-z* plane. (b) *y-z* plane. [Color figure can be viewed in the online issue, which is available at wileyonlinelibrary.com]

AR bandwidth was 902–921 MHz with a CP center frequency of 912 MHz (AR of 0.93 dB), whereas the simulated 3-dB AR bandwidth was 900–920 MHz with a CP center frequency of 910 MHz (AR of 0.72 dB). The slight discrepancy between the measurement and the simulation could be attributed to the misalignment in the placement of the dipole arms on the different sides of the substrate.

Figure 7 shows the radiation pattern of the antenna with a high symmetric profile in both the *x-z* and the *y-z* planes at 910 MHz. We note that, without the reflector, the crossed arrowhead dipole antenna radiates a bidirectional wave; the front side radiates a right-hand circular polarization (RHCP), whereas the back side radiates a left-hand circular polarization (LHCP). In particular, RHCP and LHCP can be interchanged by reversing the orientation of the vacant-quarter printed ring. The gain of the antenna was 1.4 dBic. The slight difference between the measured and the simulated LHCP patterns could be attributed to the effects of the foam rack and the tapes behind the antenna in the measurement setup. To better understand the advantages of our antenna design, performance comparison between the proposed crossed dipole and several previous designs is presented in Table 1. The proposed design has the smallest volume and the lightest weight as compared to the other designs, which is very important for handheld device applications.

TABLE 1 Comparison between the Proposed Antenna and the Other Antenna Designs

	Overall Size (mm)	$\|S_{11}\| < -10$ dB Bandwidth (MHz)	3-dB AR Bandwidth (MHz)	Gain (dBic)	Weight (g)
Proposed	60 × 60 × 0.508	851–941	902–921	1.4	~3.6
Ref. 8]	90 × 90 × 4.572	904–941	918–929	0.5	~66
Ref. 9]	90 × 90 × 4.572	904–922	908–914	3.6	~66
Ref. 10]	60 × 60 × 1.6	877–987	917–929	1.4	~11
Ref. 11]	45 × 45 × 9	912–927	906–921	2.2	~13

5. CONCLUSION

This article has introduced a lightweight crossed dipole antenna with a compact size and CP radiation for RFID in the UHF band. The proposed antenna was designed and fabricated on both sides of a thin substrate with a low density to achieve a light weight. Printed inductors were inserted in the dipole arm with a barbed-shaped end to reduce the dipole length and, consequently, to achieve a compact size. To generate the CP radiation, two dipoles were crossed through a 90° phase-delay line of a vacant-quarter printed ring, which enabled the broadband characteristic in terms of impedance and the 3-dB AR bandwidths. This antenna, exhibiting many advantages, can be widely applied to UHF RFID handheld readers.

ACKNOWLEDGMENT

This research was supported by The Ministry of Knowledge Economy, Korea, under the Information Technology Research Center support program (NIPA-2012-H0301-12-2007) supervised by the National IT Industry Promotion Agency.

REFERENCES

1. K. Finkenzeller, RFID handbook, 2nd ed., Wiley, New York, 2004.
2. E. Perret, S. Tedjini, and R. Nair, Design of antenna for UHF RFID tags, In: Proceedings of IEEE, Vol. 100, 2012, pp. 2330–2340.
3. C. Cho, H. Choo, and I. Park, Printed symmetric inverted-F antenna with a quasi-isotropic radiation pattern, Microwave Opt Technol Lett 50 (2008), 927–930.
4. J.H. Jung, H. Choo, and I. Park, Design of a U-shaped RFID tag antenna with an isotropic radiation characteristic, In: International Workshop on Antenna Technology, 2011, pp. 306–309.
5. C. Cho, H. Choo, and I. Park, Broadband RFID tag antenna with quasi-isotropic radiation pattern, Electron Lett 41 (2005), 1091–1092.
6. Y. Pan, L. Zheng, H. Liu, J. Wang, and R. Li, Directly-fed single-layer wideband RFID reader antenna, Electron Lett 48 (2012), 607–608.
7. H. Son, H. Park, K. Lee, G. Jin, and M. Oh, UHF RFID reader antenna with a wide beamwidth and high return loss, IEEE Trans Antenna Propag 60 (2012), 4928–4932.
8. Nasimuddin, Z. Chen, and X. Qing, Asymmetric-circular shaped slotted microstrip antennas for circular polarization and RFID applications, IEEE Trans Antenna Propag 58 (2010), 3821–3828.
9. Nasimuddin, Z. Chen, and X. Qing, A compact circularly polarized crossed-shaped slotted microstrip antenna, IEEE Trans Antenna Propag 60 (2012), 1584–1588.
10. Y. Wang, H. Chen, and Z. Yang, Circularly polarized crossed dipole antenna with phase delay lines for RFID handheld reader, IEEE Trans Antenna Propag 60 (2012), 1221–1227.
11. J.-H. Bang, C. Bat-Ochir, H.-S. Koh, E.-J. Cha, and B.-C. Ahn, A small and lightweight antenna for handheld RFID reader applications, IEEE Antenna Wireless Propag Lett 11 (2012), 1076–1079.
12. D. Lee, P. Park, J. Kim, and J. Choi, Aperture-coupled UHF RFID reader antenna for a handheld application, Microwave Opt Technol Lett 50 (2008), 1261–1263.
13. H.M. Chen, K.Y. Chiu, Y.F. Lin, and S.A. Yeh, Circularly polarized slot antenna design and analysis using magnetic current distribution for RFID reader applications, Microwave Opt Technol Lett 54 (2012), 2016–2023.
14. J.W. Baik, K.J. Lee, W.S. Yoon, T.H. Lee, and Y.S. Kim, Circular polarized printed crossed dipole antennas with broadband axial ratio, Electron Lett 44 (2008), 785–786.

90° BRANCH-LINE COUPLER WITH RECONFIGURABLE OUTPUT POWER RATIOS

Ariunzaya Batgerel[1] and Soon-Young Eom[2]

[1] Department of Mobile Communication and Digital Broadcasting Engineering, Daejeon, South Korea; Corresponding author: ariunzaya@etri.re.kr

[2] Department of Radio Technology Research, Smart Radio Infrastructure Research Team, Electronics and Telecommunications Research Institute, Daejeon, Korea

Received 12 December 2012

ABSTRACT: *This letter introduces a new 90° branch-line coupler with reconfigurable output power ratios (90° BC-ROPR). Unlike a conventional branch-line coupler structure, each arm of the proposed 90° BC-ROPR is defined by an asymmetrically coupled-line, and its characteristic impedance depends on the configuration of the coupled-line. The main problem that challenged this structure was unwanted loop resonance from the inner transmission lines which form a loop in a disconnected configuration. The proposed structure was designed to obtain 1:1 and 4:1 output power ratios at 3 GHz. Both the simulation and measurement results confirm that the proposed branch-line coupler successfully dealt with the loop resonance and achieved excellent performance.*

 Microwave Opt Technol Lett 55:1878–1881, 2013; View this article online at wileyonlinelibrary.com. DOI 10.1002/mop.27703

Key words: *power divider; 90° branch-line coupler; reconfigurable branch-line coupler; reconfigurable output power ratio*

1. INTRODUCTION

In recent years, reconfigurable RF and antenna systems are attracting more and more attention. To achieve such versatile systems, microwave components are also required to be reconfigurable or multifunctioning. A branch-line coupler is one of the key components in microwave circuits and used in power amplifiers, phase shifters, mixers, and array antenna feed systems.

A large number of coupler structures have been reported for unequal or arbitrary power splits, and dual or broadband characteristics [1–4]. Despite of its need in many applications, structures for a reconfigurable coupler which can provide different output power ratios are, however, less in the literature.

In this letter, we propose a new 90° branch-line coupler with reconfigurable output power ratios (90° BC-ROPR). A slot with a certain width splits each arm of the proposed structure into two parallel transmission lines creating inner and outer loops. Two bypass capacitors, four diodes, and two DC biasing circuits were used to control the proposed structure for reconfigurable outputs.

The proposed structure and its designing considerations are given in Section 2. The simulation and measurement results are discussed in Section 3. In the final section, conclusion can be found.

2. PROPOSED STRUCTURE AND DESIGNING CONSIDERATION

In Figure 1(a), a conventional 90° branch-line coupler is shown. Matched with the impedance of Z_0 at all four ports, the conventional structure obtains power split with ratio of $M{:}N$ at two output ports if the branch-line characteristic impedances, Z_1 and Z_2, satisfy the Eqs. (1) and (2), Ref. 5. The electrical length of each arm is 90° at an operating frequency, that is, $\theta_1 = \theta_2 = 90°$.